Chinese Chemical Letters 33 (2022) 643–652

Contents lists available at ScienceDirect

Chinese Chemical Letters

journal homepage: www.elsevier.com/locate/cclet

Critical review of perovskites-based advanced oxidation processes for wastewater treatment: Operational parameters, reaction mechanisms, and prospects

Ruicheng Ji[a], Jiabin Chen[a,*], Tongcai Liu[a], Xuefei Zhou[a,b,c], Yalei Zhang[a,c,*]

[a] State Key Laboratory of Pollution Control and Resources Reuse, College of Environmental Science and Engineering, Tongji University, Shanghai 200092, China
[b] Key Laboratory of Yangtze Water Environment for Ministry of Education, College of Environmental Science and Engineering, Tongji University, Shanghai 200092, China
[c] Shanghai Institute of Pollution Control and Ecological Security, Tongji University, Shanghai 200092, China

ARTICLE INFO

Article history:
Received 2 April 2021
Revised 5 June 2021
Accepted 16 July 2021
Available online 21 July 2021

Keywords:
Perovskite
Advanced oxidation processes
Wastewater
Peroxide
Free radical

ABSTRACT

In the field of advanced oxidation processes (AOPs) of wastewater, many materials can be used as heterogeneous catalysts. The role of these catalysts is to activate oxidants and generate reactive oxygen species (ROS) to decompose refractory pollutants. Perovskite oxide, an emerging catalyst in the field of AOPs, has been extensively studied in wastewater treatment. Nevertheless, the application of perovskite in AOP systems still faces some problems, such as leaching of metal ions, a small surface area, a low number of active sites, *etc.* Herein, this critical review comparatively examines the activation mechanisms of peroxymonosulfate, hydrogen peroxide, and peroxydisulfate. Furthermore, the formation pathways of oxidizing species based on recent advances in experimental and theoretical studies were evaluated. In addition, the impacts of water parameters and constituents such as initial pH, oxidant concentration, catalyst dosage, natural organic matter, halide, phosphate, and carbonate were discussed. Finally, a critical discussion and prospects of mechanism exploration and possible materials development are proposed to confront the existing challenges in the application of perovskite oxides in AOPs.

1. Introduction

With the rapid development of human society, water pollution has become more and more complex. Conventional wastewater treatment methods have trouble treating emerging and refractory pollutants (such as pharmaceuticals, personal care products, pesticides, herbicides, dyes). Advanced oxidation processes (AOPs) have been regarded as an efficient advanced treatment technology to produce reactive oxygen species (ROS) with high redox potential and decompose pollutants in water.

Peroxide derivatives consisting of peroxide bonds (O—O) have been extensively employed as the precursors of ROS in AOPs. Among them, peroxymonosulfate (PMS), peroxydisumphate (PDS), and hydrogen peroxide (H_2O_2) have attracted extensive attention and have been widely researched. In AOP systems based on peroxides, the main ROS are free radicals, which have a high reactivity and a short half-life [1-9]. Wherein, hydroxyl radicals ($^{\bullet}OH$), sulfate radicals ($SO_4^{\bullet-}$), superoxide radicals ($O_2^{\bullet-}$), peroxyhydroxy radical ($HO_2^{\bullet}$) *etc.*, are the most common free radicals. However, there are also non-radical ROS that's generated in some systems, such as singlet oxygen ($^1O_2$).

Transition metal ions (especially Co, Fe, Cu, Mn, *etc.*) have been employed as the most effective activators for the activation of persulfate (including PMS and PDS) and H_2O_2. However, the key problem of homogeneous reactions is the secondary pollution caused by the toxic metal ions. In addition, the free ions used as catalysts are difficult to recover, which is not economical. Therefore, heterogeneous catalytic systems are more promising [10-12]. In heterogeneous catalytic systems, electron (e^-) transfer between metal oxides and peroxides take place at the interface to produce ROS [13-16]. Nevertheless, the catalytic activity of single-metal oxides is limited by the surface area and the number of active sites. To solve these problems, researchers doped different metals with single metal oxides. The synergistic effect between different metals, the improvement of electronic structure and oxygen vacancy concentration make multi-metal oxides better catalysts [17-19]. As one

* Corresponding author.
E-mail addresses: chenjiabincn@163.com (J. Chen), zhangyalei@tongji.edu.cn (Y. Zhang).

https://doi.org/10.1016/j.cclet.2021.07.043
1001-8417/

kind of multi-metal oxide, perovskite demonstrates the advantages of having a stable structure and diverse composition.

Perovskite has the general formula ABO_3, wherein A-site ions generally are rare earth or alkaline earth elements; B-site ions usually are transition metal elements. At present, perovskites are mainly prepared by the sol-gel method [20-24], combustion [25], co-precipitation [26], chelating precursor method [27], and other methods [28,29]. The structure of perovskite can be regarded as a BX_3 octahedron building with A cations introduced in it [30,31]. Because of the fluctuation of the cation radius, the crystal can deviate from the ideal structure within a certain extent [32]. Thus, both A-site and B-site ions can be partially replaced by other metal ions with similar radii and their crystal structure can remain unchanged. Due to this characteristic, over 90% of the elements in the periodic table can stably exist in the perovskite structure [31]. The unique structure of perovskite gives it its distinctive properties, such as its ferroelectricity [33], ferromagnetism [34,35], multiferroicity [36], piezoelectricity [37,38], superconductivity [39,40], as well as its electrocatalytic [41,42], and photocatalytic properties [43,44]. More importantly, the perovskite structure allows special introduction of desired metal ions into the B-site to enhance catalytic efficiency. Besides, the high thermal and hydrothermal stability of the structure make it possible for perovskites to work stably under various conditions. Therefore, perovskite can be a promising activator of peroxide in AOPs. The advanced oxidation processes, which use perovskite as heterogeneous catalyst to activate oxidants, generate ROS, and degrade pollutants was called perovskite-based AOPs.

Herein, the present review focuses on recent studies in materials design, characterizing the catalytic activity, identifying the reactive species, and investigating the factors (reaction temperature, initial pH, oxidant concentration, catalyst dosage, co-existing compounds) which affect the reaction efficiency. In addition, reaction mechanisms (radical and/or nonradical) are probed by means of both experimental and theoretical investigations. At last, the research gaps of perovskite-based AOPs are detailed, and opportunities are proposed for further mechanistic investigations with advanced strategies and applications of perovskite oxide catalysis during catalytic oxidation.

2. Perovskite-based AOPs for water decontamination

Emerging and refractory pollutants are increasing in water environments. Perovskite-based AOPs are considered to be an effective treatment method for water contaminated by these pollutants. Therefore, more and more new studies focus on perovskite-based AOPs for the decontamination of water. To get a general understanding, we summarized some correlative studies and listed their crucial information in Table 1.

In the perovskites used in these studies, the metal elements on the A-sites were rare earth or alkali earth metal such as La, Sr, Bi, Ca, and Ba. Among them, La was the most common, and Bi often appeared in the photocatalytic reaction. The transition metal elements on the B-sites varied, including Co, Fe, Cu, Mn, Ti, *etc.* Wherein, Co was the most efficient and the most common metal; Fe was the most typical metal in Fenton reaction. Overall, lanthanum-based perovskites ($LaBO_3$), cobalt-based perovskites ($ACoO_3$), and iron-based perovskites ($AFeO_3$) received the most attention.

Based on the conventional ABO_3 structure, researchers carried out a series of modifications to improve the catalytic performance of perovskites. One method is to change the surface properties of perovskites. By doping different metal ions, the electronic structure, oxygen vacancy concentration, metal-oxygen bond strength, and lattice structure of perovskites can be controlled [17], more low-valence B-site transition metal active sites can be produced [18], and synergistic effects between different metals can be observed [19]. Another method involves expanding the surface area. The perovskites prepared by conventional methods have a close-packed morphology, which limits the catalytic activity [45,46]. Previous studies expanded the catalyst surface area by preparing nano-scaled perovskite with different configurations or by compositing perovskite with other materials. For nano-scaled perovskite, nanoparticle is the most common configuration. Beside, perovskites with the configurations of nanofiber [46] and hollow fiber membrane [47] were also prepared. In regard to the materials for modification, single-component metallic materials, nonmetallic materials and natural minerals have been reported. In metallic materials, metal oxides are most commonly used, such as ZrO_2 [45], CeO_2 [48], LaO_3 [18], Al_2O_3 [49] and TiO_2 [50]. In addition to metal oxides, Ming Zhu *et al.* [17] made CoOOH nanoflakes grow on the surface of perovskite. In nonmetallic materials, carbon sphere [51,52], mesoporous/macroporous SiO_2 [53] and g-C_3N_4 [54] have been reported. In addition, as a natural mineral, montmorillonite [54] has also been applied.

In these perovskite-based AOPs systems, PMS and H_2O_2 have often been selected as ROS precursors while PDS had relatively few applications. Moreover, the target pollutants were primarily classified into four groups: Aromatic compounds (represented by phenol); dyes (represented by rhodamine B); pharmaceuticals and personal care products (represented by carbamazepine), and herbicides (represented by atrazine).

As for the reaction conditions, most of the studies performed reactions at room temperature to simulate environmental conditions. Part of the systems are combined with light, ultrasound, electricity, and microwave to promote the reaction efficiency. For photocatalytic systems, the low bandgap energy of perovskites makes it possible for most systems to use visible light as a light source. When perovskites were composited with the photocatalyst titanium dioxide (TiO_2) with a high bandgap energy, UV was also used as a light source [50,55,56]. Sonolysis systems were usually combined with Fenton systems to generate more $^{\bullet}OH$ radicals. The combination with electrochemical systems was scarcely reported in the literature. Microwave was used to induce H_2O_2 to trigger thermal and non-thermal effects, which can enhance the degradation of organic pollutants. However, microwave absorbing catalysts are essential in such systems. Thus the combination of microwave and perovskites is logical.

In the perovskite-based AOPs, different ROS involved (including free radicals and $^1O_2$) were clarified by electron paramagnetic resonance (EPR). Firstly, specific spin trapping agents captured ROS to form adducts. For example, 5,5-dimethyl-1-pyrroline (DMPO) was used to capture $^{\bullet}OH$, $SO_4^{\bullet-}$, and $O_2^{\bullet-}$, and $^1O_2$ was captured by 2,2,6,6-tetramethyl-4-piperidone (TEMP) [57-60]. Then the signals were detected and identified by EPR spectrometer. Except for EPR, quenching agents (such as ethanol (EtOH), *tert*-butyl alcohol (TBA), sodium azide (NaN_3) and furfuryl alcohol (FFA) [10,57]) were added to the reaction system to investigate the contribution of each ROS and probe the dominant ROS in the reaction. In most PMS and PDS systems, $SO_4^{\bullet-}$ was the dominant ROS, while $^{\bullet}OH$ also contributed to the reaction. In H_2O_2 systems, $^{\bullet}OH$ was the dominant ROS, and other free radicals such as $HO_2^{\bullet}$ and $O_2^{\bullet-}$ also participated in the reaction. Meanwhile, some reaction systems generated $^1O_2$ as the dominant ROS [18,57-59,61] or as the assistant of the free radicals to decontaminate water [17,62-64].

As a heterogeneous catalyst, ion leaching and recycling of perovskite must be considered in practical application. The long time contact between perovskite and water phase inevitably leads to ion leaching. For perovskite, ion leaching can change its surface chemical composition, damage its crystal framework, and reduce its catalytic activity, which is also one of the factors affecting the reusability [65]. It is worth noting that due to the strong toxicity

Table 1
Summary of the perovskite-based advanced oxidation processes in recent studies.

Perovskite catalyst	Oxidant	Target pollutant	Degradation effect [a]	Reaction conditions	Ref.
$PrBaCo_2O_{5+\delta}$	PMS	Phenol (20 mg/L)	k = 0.144 min^{-1}	[catalyst] = 0.1g/L; [PMS] = 2.0g/L	[10]
$LaBO_3$(B = Co/Cu/Fe/Ni)	PMS	Rhodamine B (10 mg/L)	k = 0.062/0.016/0.011/0.011 min^{-1} (M = Co/Ni/Co/Fe)	[catalyst] = 100mg/L; [PMS] = 100 mg/L	[12]
$LaBO_3$ (B = Ni/Mn/Fe) [b]	PMS	Ofloxacin (10 mg/L)	k = 0.239/0.083/0.0049 min^{-1} (B = Ni/Mn/Fe)	[catalyst] = 0.1g/L; [PMS] = 0.5 g/L; pH 7	[57]
$LaFeO_3$	PMS	Diclofenac (0.025 mmol/L)	100% (30 min)	[catalyst] = 0.1g/L; [PMS] = 0.5 mmol/L; pH 7.0	[79]
$La_{0.4}Sr_{0.6}MnO_{3-\delta}$ [b]	PMS	Phenol (0.2 mmol/L)	k = 0.0308 min^{-1}	[catalyst] = 0.2g/L; [PMS] = 6.5 mmol/L;	[58]
$SrCo_{1-x}Ti_xO_{3-\delta}$	PMS	Phenol (20 mg/L)	k = 0.056 mg L^{-1} min^{-1}	[catalyst] = 0.1g/L; [PMS] = 2 g/L;	[65]
$LaCo_{1-x}Mn_xO_{3-\delta}$	PMS	Phenol (20 ppm)	k = 0.053 min^{-1}	[catalyst] = 0.1g/L; [PMS] = 2.0 g/L; pH 6.7	[67]
$La_{1.15}MnO_{3+\delta}$ [c]	PMS	Rhodamine B (20 ppm)	k = 0.086 min^{-1}	[catalyst] = 0.2 g/L; [PMS] = 0.8 g/L; pH 4.65	[64]
$LaCoO_3/ZrO_2$	PMS	Rhodamine B (10 mg/L)	k = 0.171 min^{-1}	[catalyst] = 100 mg/L; [PMS] = 100 mg/L	[45]
$CoTiO_3$ (nanofiber)	PMS	Amaranth (50 mg/L)	k = 0.870 min^{-1}	[catalyst] = 100 mg/L; [PMS] = 100 mg/L	[46]
$CoTiO_3$	PMS	Acid azo dyes (50 mg/L)	k = 0.278/0.272/0.109 min^{-1} AR27/AY17/AB120	[catalyst] = 100 mg/L; [PMS] = 100 mg/L; pH 7.0	[71]
$LaCoO_3$-TiO_2	PMS	Herbicide (10 mg/L)	k = 6.0 ± 0.3/3.1 ± 0.4/0.55 ± 0.08/2.1 ± 0.2 L mol^{-1} min^{-1}; (metazachlor/tembotrione tritosulfuron/ethofumesate)	[catalyst] = 0.5 g/L; [PMS] = 0.15 mmol/L; pH 7.0; UV light	[55]
$SrCo_{0.6}Ti_{0.4}O_{3-\delta}$@CoOOH [c]	PMS	Phenol (20 mg/L)	k = 0.84 mg L^{-1} min^{-1}	[catalyst] = 0.06 g/L; [PMS] = 2.0 g/L	[17]
$LaCoO_3$	PMS	Herbicide (1 mg/L)	100% (1 min)/ 100% (1 min)/ 100% (1 min)/ 90% (100 min) (metazachlor/tembotrione /ethofumesate/ tritosulfuron)	[catalyst] = 0.5 g/L; [PMS] = 0.1 mmoil/L; pH 3-5	[78]
$ACoO_3$ (A=La, Ba, Sr, Ce)	PMS	Phenol (20 mg/L)	100%/95%/84%80% (180 min) (A = Sr/La/Ba/Ce)	[catalyst] = 0.2 g/L; [PMS] = 0.1 mmol/L; nature pH	[77]
Sr_2CoFeO_6	PMS	Bisphenol F (20 mg/L)	k = 0.012 min^{-1}	[catalyst] = 0.3 g/L; [PMS] = 0.1 mmol/L; pH 7; UV light	[72]
$LaCo_{1-x}Cu_xO_3$ [c]	PMS	Phenol (20 mg/L)	k = 0.302 min^{-1}	[catalyst] = 0.10 g/L; [PMS] = 0.20 g/L	[62]
$BiFe_{1-x}Mn_xO_3$	PMS	Bisphenol A (50 mg/L)	100% (35 min/25 min/15 min); (0%/5%/10%Mn doped)	[catalyst] = 0.45 g/L; [PMS] = 0.10 mmol/L; pH 2.5; visible light	[73]
Ag-$La_{0.8}Ca_{0.2}Fe_{0.94}O_{3-\delta}$ (hollow fibre membrane)	PMS	Methylene Blue (10 ppm)	90% (75 min)	[PMS] = 0.6 mmol/L	[47]
$Ba_{0.5}Sr_{0.5}Co_{0.8}Fe_{0.2}O_{3-\delta}$	PMS	Phenol (40 mg/L)	k = 0.032 min^{-1}	[catalyst] = 0.1 g/L; [PMS] = 6.5 mmol/L; pH 8.0	[2]
$LaMnO_3$ [b]	PMS	Ofloxacin/Phenol (10 mg/L/)/(20 mg/L)	k = 0.088/0.042 min^{-1} (Ofloxacin/Phenol)	[catalyst] = 0.2 g/L; [PMS] = 0.5 g/L; pH 6.0	[59]
$LaCoO_3$	PMS	2-phenyl-5-sulfobenzimidazole (5 mg/L)	100% (4.5 min);	[catalyst] = 500 mg/L; [PMS] = 5.0 mmol/L; pH 2.5	[26]
$LaFeO_3$	PMS	Diclofenac (0.025 mmol/L)	k = 0.0833 min^{-1}	[catalyst] = 0.1 g/L; [PMS] = 0.5 mmol/L; pH 7.0	[87]
Ag-$La_{0.8}Ca_{0.2}Fe_{0.94}O_{3-\delta}$	PMS	Methylene Blue (10 mg/L)	90%(45 min)	[catalyst] = 1.0 g/L; [PMS] = 0.24 g/L; pH 5.5	[60]
$CaCu_3Ti_4O_{12}$	PMS	Ibuprofen (20 mg/L)	91% (30 min)	[catalyst] = 20 mg/L; [PMS] = 0.5 mmol/L; pH 7.0; visible light	[93]
$LaCoO_3/Al_2O_3$	PMS	Atrazine (5 mg/L)	100% (30 min)	[catalyst] = 100 mg/L; [PMS] = 100 mg/L; pH 6.8	[49]
$LaFe_{1-x}Cu_xO_{3-\delta}$	PMS	Atrazine (23 μmol/L)	k = 0.0405 min^{-1}	[catalyst] = 0.5 g/L; [PMS] = 0.5 mmol/L; pH 6.1	[19]
$LaCoO_3$	PMS	Carbamazepine (21.16 μmol/L)	k = 0.26 min^{-1}	[catalyst] = 0.05 g/L; [PMS] = 0.5 mmol/L; pH 6.0	[69]
$La_{0.4}Sr_{1.05}MnO_x$ [b]	PMS	Phenol (20 ppm)	k = 0.07006 min^{-1}	[catalyst] = 0.2 g/L; [PMS] = 2 g/L	[61]
$La_{0.5}Sr_{0.5}FeO_3$	PMS	2,4-dichlorophenoxyacetic acid (10 mg/L)	k = 0.072 min^{-1}	[catalyst] = 0.6 g/L; [PMS] = 1 mmol/L; pH 4.65	[63]
$BiFeO_3$	PMS	Rhodamine B (5 mg/L)	k = 0.026 min^{-1}	[catalyst] = 5 mmol/L; [PMS] = 5 mmol/L; visible light	[66]

(*continued on next page*)

Table 1 (*continued*)

Perovskite catalyst	Oxidant	Target pollutant	Degradation effect [a]	Reaction conditions	Ref.
$Co/BiFeO_3$	PDS	Tetracycline (10 mg/L)	81.09% (55 min)	[catalyst] = 0.5 g/L; [PDS] = 3.33g/L;	[11]
$La_{0.7}Sr_{0.3}MnO_3$	PDS	Methyl Orange (13 ppm)	k = 0.103 min^{-1}	[catalyst] = 25 mg/L; [PDS] = 2.5 mmol/L; pH 1.4	[68]
CeO_2-$LaMO_3$ (M = Cu, Fe)	H_2O_2	Bisphenol F (20 mg/L)	k = 0.07410 min^{-1}	[catalyst] = 0.4 mg/L; [H_2O_2] = 12.5 mmol/L;	[48]
$LaAl_{0.95}Cu_{0.05}O_3$	H_2O_2	2-Chloroprocaine (10 mg/L)	100% (120 min)	[catalyst] = 1g/L; [H_2O_2] = 10 mmol/L	[89]
LaO_3-$LaFeO_3$ [b]	H_2O_2	Methyl orange (5 ppm)	k = 0.0402 min^{-1}	[catalyst] = 0.5 g/L; [H_2O_2] = 0.198 mol/L; pH 3	[18]
$LaFeO_3$	H_2O_2	Bisphenol A (15 ppm)	21.8% (3 h);	[catalyst] = 0.5 g/L; [H_2O_2] = 2.38 mmol/L; pH 6.7; visible light; ultrasound	[94]
$LaFeO_3$/C	H_2O_2	Rhodamine B (15 mg/L)	85.5% (100 min)	[catalyst] = 1 g/L; [H_2O_2] = 0.192 mol/L; visible light	[51]
$LaFeO_3$	H_2O_2	Bisphenol A (15 ppm)	21.8% (3 h);	[catalyst] = 0.5 g/L; [H_2O_2] = 2.38 mmol/L; pH 6.7; visible light; ultrasound	[95]
Sr_2FeCuO_6	H_2O_2	Cotinine (50 mg/L)	k = 0.00397 min^{-1}	[catalyst] = 0.2g/L; [H_2O_2](electrogenerated); pH 3.0; [Na_2SO_4] = 0.05 mol/L (supporting electrolyte); electrochemical system	[81]
$LaCu_{1-x}M_xO_3$ (M = Mn/Ti)	H_2O_2	Paracetamol (50 mg/L)	90% (5 h)/87% (5 h) (M = Mn/Ti)	[catalyst] = 0.2 g/L; [H_2O_2] = 13.8 mmol/L;	[70]
$LaTi_{0.4}Cu_{0.6}O_3$	H_2O_2	Rhodamine B (8 mg/L)	94% (120 min)	[catalyst] = 1.4 g/L; [H_2O_2] = 20 mmol/L;	[83]
$LaFeO_3$	H_2O_2	Sulfamethoxazole (3 mg/L)	k = 0.029 min^{-1}	[catalyst] = 1.4 g/L; [H_2O_2] = 23 mmol/L; pH 6.48	[86]
$BiFe_{0.8}Cu_{0.2}O_3$:	H_2O_2	Phenol (10 mg/L)	k = 0.016 min^{-1};	[catalyst] = 0.5 g/L; [H_2O_2] = 10 mmol/L; pH 4.0	[84]
$AFeO_3$ (A = La/Bi)	H_2O_2	Phenol (25 mg/L)	k = 0.13/0.15 h^{-1}(A = La/Bi)	[catalyst] = 0.1 g/L; [H_2O_2] = 3 g/L; pH 7.0	[74]
$LaCuO_3$	H_2O_2	Tartrazine (100 ppm)	46.6% (120min)/64.4% (120 min) (visible light/UV)	[catalyst] = 0.25 g/L; [H_2O_2] = 8 mmol/L; pH 3.0; visible light/UV light	[75]
$LaBO_3$ (B = Cu, Fe, Mn, Co, Ni)	H_2O_2	Phenol (10 mmol/L)	100% (2.5 h)/81% (10 h) (B = Cu/Fe)	[catalyst] = 0.5 g/L; [H_2O_2] = 0.7 mol/L; pH 3.0	[76]
$LaFeO_3$/mesoporous/macroporous silica	H_2O_2	Rhodamine B (20 mg/L)	k = 0.0367 min^{-1}	[catalyst] = 1.0 g/L; [H_2O_2] = 10 mmol/L; pH 6.0; visible light	[53]
$LaFeO_3$ nanocrystalline	H_2O_2	Phenol (50 mg/L)	92% (360 min)	[catalyst] = 3.0 g/L; [H_2O_2] = 8.82 mmol/L; pH 4.0; visible light	[80]
$CeMg_xFe_{1-x}O_{3-\delta}$	H_2O_2	Methylene Blue (25 ppm)	99% (180 min)	[catalyst] = 1.0 g; visible light	[23]
$LaFeO_3$	H_2O_2	Bisphenol A (66 μmol/L)	90.8% (6 h)	[catalyst] = 0.5 g/L; [H_2O_2] = 2.4 mmol/L; pH 8.5; ultrasound	[82]
$La_xTi_yFeO_3$	H_2O_2	4-Chlorophenol (25 mg/L)	k = 0.025 min^{-1}	[catalyst] = 0.5 g/L; [H_2O_2] = 125 mg/L; UV light	[24]
$LaCu_{0.5}Co_{0.5}O_3$/Montmorillonite /g-C_3N_4	H_2O_2	Bisphenol A (50 mg/L)	98.7% (2 min)	[catalyst] = 0.2 g/L; [PMS] = 2 g/L; microwave	[54]
xCe/$LaCo_{0.5}Cu_{0.5}O_3$@carbon sphere	H_2O_2	Salicylic acid (50 mg/L)	k = 0.687 min^{-1}	[catalyst] = 6.0 g/L; [H_2O_2] = 2 mL/L; pH 6.0; microwave	[52]
$TiO_2/SrTiO_3$	H_2O_2/PDS	4-Nitrophenol (10 ppm)	k = 0.0277 min^{-1}	[catalyst] = 0.1 g/L; [H_2O_2] = 10 ppm/[PDS] = 10 ppm; pH 4.0; UV light	[50]
$LaFeO_3$	H_2O_2/PDS	4-Chlorophenol (9 ppm)	97% (60 min)	[catalyst] = 0.5 g/L; [PDS] = 1.0 mmol/L; ultrasound	[85]

[a] Degradation effect was expressed by rate constants (k) or degradation efficiency (%) within a certain period.
[b] Singlet oxygen ($^1O_2$) is generated in this study and is the dominant reactive oxygen species (ROS).
[c] Singlet oxygen ($^1O_2$) is generated in this study but not the dominant reactive oxygen species (ROS).

of cobalt ions, the leaching control of cobalt-containing perovskites has become a common concern [10]. According to the existing experiments on perovskite recyclability, after several consecutive cycles runs, catalytic performance of perovskite is slightly weakened, which is due to ion leaching of perovskite and poisoning of active sites by organic matters [58,62,65-70]. However, despite the reduction, the catalytic activity of perovskite is still nonnegligible. The characterization methods show that the crystal structure of perovskite does not change before and after the reaction, which indicates that perovskite had good stability and reusability [62,71,72].

3. Influencing factors of reactivity

3.1. Effect of temperature

Many studies showed that reaction temperature had a significant effect on degradation kinetics [12,18,45,46,48,55,59,62,71-76]. Increasing temperature significantly enhanced the effect of oxidant activation and accelerated the removal of pollutants [59,62]. Firstly, higher temperature led to an increase in the diffusion and adsorption rate of pollutants [72]. Meanwhile, higher temperature provided more energy for the cleavage of O—O bonds, thereby promoting the production of free radicals [66]. For example, PMS can self-decompose to generate more $^{\bullet}OH$ under high-temperature conditions (Eq. 1) [62,72].

$$HSO_5^- + \text{heat} \rightarrow SO_4^{\bullet -} + {}^{\bullet}OH \quad (1)$$

Arrhenius equation (Eq. 2) is an empirical formu demonstrating ing the relationship between the chemical reaction rate constant and temperature. Linearizing the Arrhenius equation and fitting experimental data achieved a good fitting result, which indicated that most reaction systems could use the Arrhenius equation to correlate degradation kinetics with temperature. Therefore, it is reasonable to use this method to predict the rate constants at different temperatures. Among the trials, the degradation rate constant (k) increased with increasing temperature (T).

$$k = A\exp(-E^a/RT) \quad (2)$$

wherein, E_a is the activation energy of degradation (kJ/mol), A is the pre-exponential factor (min^{-1}), R is the universal gas constant, and T is the temperature (K).

In practical applications, maintaining a high temperature to optimize the reaction costs a large amount of energy, which is not economical. The exception is dyeing wastewater, which can maintain a high reaction temperature. A high temperature effectively utilizes thermal energy and improves reaction efficiency [75].

3.2. Effect of initial pH

The effect of the initial pH on the perovskite-based AOPs was quite significant. The initial pH not only affected the existent forms of pollutants, peroxides and ROS in the matrix, but it also affected the surface electrical properties and ion leaching amount of the catalyst, thereby changing the reaction efficiency.

3.2.1. Effect of initial pH on reactive oxygen species

At different initial pH, hydrogen ions (H^+) or hydroxide ions (OH^-) directly affected the reaction activity by generating, scavenging, and converting ROS.

In a study conducted by Jie Miao *et al.* [58], under acidic (pH 3.2) and basic conditions (pH 9.2), H^+ and OH^- helped generate $^1O_2$ (Eqs. 3-8).

$$HSO_5^- + H_2O \xrightarrow{OH^-} H_2O_2 + HSO_4^- \quad (3)$$

$$H_2O_2 \xrightarrow{OH^-} H^+ + HO_2^- \quad (4)$$

$$H_2O_2 \rightarrow 2{}^{\bullet}OH \quad (5)$$

$$HO_2^- \rightarrow H^+ + O_2^{\bullet -} \quad (6)$$

$$O_2^{\bullet -} + {}^{\bullet}OH \rightarrow {}^1O_2 + OH^- \quad (7)$$

$$2O_2^{\bullet -} + 2H^+ \rightarrow H_2O_2 + {}^1O_2 \quad (8)$$

Under low pH conditions, the high concentration of H^+ in the solution may decrease the number of free radicals (Eqs. 9 and 10) [17,49,67].

$$^{\bullet}OH + H^+ + e^- \rightarrow H_2O \quad (9)$$

$$SO_4^{\bullet -} + H^+ + e^- \rightarrow HSO_4^{\bullet -} \quad (10)$$

Both $SO_4^{\bullet -}$ and $SO_5^{\bullet -}$ can be converted to $^{\bullet}OH$ under high pH conditions (Eqs. 11 and 12) [2,17,49,65,67,77].

$$SO_4^{\bullet -} + OH^- \rightarrow SO_4^{2-} + {}^{\bullet}OH \quad (11)$$

$$2SO_5^{\bullet -} + 2OH^- \rightarrow 2SO_4^{2-} + 2{}^{\bullet}OH + O_2 \quad (12)$$

3.2.2. Effect of initial pH on catalysts

The initial pH can affect the surface charge of the catalyst, which will affect the adsorption and binding capacity with oxidants and pollutants [2]. The pH at zero charge on the perovskite surface is called the isoelectric point (pH_{pzc}). When $pH < pH_{pzc}$, the surface of the perovskite is positively charged; otherwise, it is negatively charged.

Many perovskites have a pH_{pzc} higher than 7.0 (*e.g.*, $LaCoO_3$-9.08 [78], Sr_2CoFeO_6-8.70 [72], $LaCo_{0.4}Cu_{0.6}O_3$-10.92 [62], $LaCuO_3$-7.60 [75], $LaFeO_3$-9.30 [79]). Thus, at low initial pH values, the perovskites are more likely to be positively charged. Moreover, HSO_5^- and $S_2O_8^{2-}$ are easier to be adsorbed on the perovskite surface, thereby promoting the activation efficiency. At the same time, positively charged catalysts also facilitate the adsorption of negatively charged anionic contaminants, such as azo dyes [18,75,80].

Besides, at certain pH, ions can deposit on the surface of the catalyst and affect the surface electrical properties. For example, a large number of OH^- will deposit on the perovskite surface and make it negatively charged, which hinders some negative groups from approaching [12,45,46,71].

3.2.3. Effect of initial pH on oxidant

The initial pH can affect the form and stability of the oxidant. For PMS, the ionization constants of H_2SO_5 are $pK_{a1} < 0$ and $pK_{a2} = 9.4$. Under acidic or neutral conditions, PMS mainly exists as HSO_5^- in solution, which is easier to be adsorbed and activated on the positively charged catalyst surface [19,49,62,72,79]. Under alkaline conditions, PMS mainly exists in the form of SO_5^{2-}, which is less active [19,49].

In addition, pH affects the stability of PMS. At low pH values, hydrogen bonds will form between H^+ ions and O—O groups of HSO_5^-. This phenomenon weakens the negative charge of HSO_5^- and inhibits its interaction with positively charged catalysts [79]. Therefore, PMS is more stable and less likely to be activated [12,45,46,71]. Under alkaline conditions, PMS will self-decompose without generating ROS, which also influences the reaction [46,71,72,77].

For H_2O_2, when $pH < 3$, H_2O_2 will combine with H^+ to form $H_3O_2^+$ (Eq. 13), which is harder to activate [18,53,81]. With the increase of pH, H_2O_2 becomes more active and begins to decompose to H_2O and O_2 (Eq. 14) [53,82].

$$H_2O_2 + H^+ \rightarrow H_3O_2^+ \quad (13)$$

$$2H_2O_2 \rightarrow 2H_2O + O_2 \quad (14)$$

3.2.4. Effect of initial pH on metal ion leaching

It is quite certain that metal ion leaching is more severe at lower initial pH. This is because the acidic solution will corrode the perovskites and release the metal ions. Free metal ions will act as a homogeneous catalyst [2,72,78]. Although the reaction rate may increase, the strong toxicity of metal ions will cause severe pollution

to the environment. Thus, it is necessary to control the solution to neutral or alkaline to reduce leaching [10,65,67,72].

3.3. Effect of oxidant concentration

At the beginning of the increase of the oxidant concentration, the degradation rate constant improved significantly. This phenomenon was because more oxidants were used as precursors to produce ROS [12,55,66,77,78].

When the oxidant concentration reached a higher level, the reaction efficiency stopped improving or was even suppressed. This phenomenon was attributed to the limited catalyst which could not provide enough active sites, thereby limiting the improvement of the degradation efficiency. Moreover, the excess of oxidants adversely affected the reaction (PMS will convert $SO_4^{\bullet-}$ to less active $SO_5^{\bullet-}$ (Eq. 15) [19,49,62,72,79]; H_2O_2 will compete with target contaminants to react with $^{\bullet}OH$ (Eq. 16) [48,53,74,75,83,84].

$$2HSO_5^- + SO_4^{\bullet-} \rightarrow SO_5^{\bullet-} + SO_4^{2-} + H^+ \quad (15)$$

$$H_2O_2 + {}^{\bullet}OH \rightarrow H_2O + HO_2^{\bullet} \quad (16)$$

3.4. Effect of catalyst dosage

At lower catalyst dosages, the optimal dosage and highest reaction efficiency have not been achieved [12,78]. Therefore, increasing the catalyst dosage provided a larger surface area and more active sites, which facilitated the adsorption and binding with the oxidant, thereby producing more free radicals and improving the degradation efficiency.

However, when the catalyst dosage reaches a certain level, the addition of catalyst no longer improved the degradation efficiency [19,49,62,68,72,74,77,81,82] and even inhibited it [48,53,79,84,85]. The reasons for the inhibition are fourfold: (1) Excessive perovskite particles aggregate and decrease the surface area [72]. (2) Excessive metal active sites scavenge free radicals [48,62,72,75,77,79,81,84,85]. (3) In systems with light irradiation, perovskite particles increase the solution turbidity and scatter the light, thereby reducing the intensity of the irradiation field. (4) In systems with ultrasound, perovskite particles obstruct the distribution of sound waves and reduce the energy input into the system.

3.5. Effect of co-existing compounds

The composition of the wastewater is complicated. Salts, organic matter, and other substances will all affect the reaction. Therefore, the influence of co-existing compounds on the reaction becomes a common concern.

(1) Coexisting anions: According to current studies, the effect of chloride ions (Cl^-) depends on the concentration and pollutant type. When the Cl^- concentration is low (compared with the pollutant concentration), the effect on the reaction is negligible [12,45,58,72,79,86]. When the Cl^- concentration reaches a high level, it begins to affect the reaction.

In most situations, Cl^- hurts the reaction. This is due to the production of chlorine free radicals ($Cl^{\bullet}/Cl_2^{\bullet-}$) [12,17,46,71,79], chlorine (Cl_2) and hypochlorous acid (HOCl) [67,73] (Eqs. 17–20) with lower oxidation potential. In contrast, when phenol is the target pollutant, Cl^- promotes the reaction. The positive effect is attributed to the stronger selectivity of $Cl^{\bullet}/Cl_2^{\bullet-}$. These radicals can effectively attack electron-rich compounds or groups [79]. Coincidentally, phenol is an aromatic compound with a hydroxyl group. Electron donors will continuously supply charges to the benzene ring with a high charge density. Therefore, $Cl^{\bullet}/Cl_2^{\bullet-}$ will react with phenol faster than $^{\bullet}OH$ and $SO_4^{\bullet-}$ [17]. However, in the reaction system with $^1O_2$ as active oxygen, the effect of Cl^- is not obvious [18,59].

$$2Cl^- + HSO_5^- + H^+ \rightarrow Cl_2 + SO_4^{2-} + H_2O \quad (17)$$

$$Cl^- + HSO_5^- \rightarrow HOCl + SO_4^{2-} \quad (18)$$

$$Cl^- + SO_4^{\bullet-} \rightarrow Cl^{\bullet} + SO_4^{2-} \quad (19)$$

$$Cl^- + Cl^{\bullet} \rightarrow Cl_2^{\bullet-} \quad (20)$$

Bicarbonate/carbonate ions (HCO_3^-/CO_3^{2-}) which can transform into each other [73] exhibit a significant inhibition in perovskite-based AOPs (including the systems that produce $^1O_2$) [17,58,59,72,73,86,87]. Higher concentrations lead to more obvious inhibition [59,72]. HCO_3^-/CO_3^{2-} will act as radical quenchers and generate less active $HCO_3^{\bullet}/CO_3^{\bullet-}$ (Eqs. 21-24) [17,49]. Besides, $HCO_3^{\bullet}/CO_3^{\bullet-}$ is easily adsorbed on the positively charged catalysts and competes with oxidants [87].

$$CO_3^{2-} + SO_4^{\bullet-} \rightarrow CO_3^{\bullet-} + SO_4^{2-} \quad (21)$$

$$HCO_3^- + SO_4^{\bullet-} \rightarrow HCO_3^{\bullet} + SO_4^{2-} \quad (22)$$

$$CO_3^{2-} + {}^{\bullet}OH \rightarrow CO_3^{\bullet-} + OH^- \quad (23)$$

$$HCO_3^- + {}^{\bullet}OH \rightarrow CO_3^{\bullet-} + H_2O \quad (24)$$

Phosphate/ hydrogen phosphate /dihydrogen phosphate (PO_4^{3-}/HPO_4^{2-}/$H_2PO_4^-$) is another group of ions that significantly inhibits the reaction [59,79,86]. The ionization constants of phosphoric acid (H_3PO_4) are listed as follows: $pK_{a1} = 2.12$, $pK_{a2} = 7.21$, and $pK_{a3} = 12$. When pH = 7.0, $H_2PO_4^-$ and HPO_4^{2-} are the main forms in solution. They are easy to chelate with the catalysts and hinder the reaction between the catalyst and the oxidant [49,79]. At the same time, $H_2PO_4^-$ is an effective quencher of $^{\bullet}OH$ (Eq. 25) [49].

$$H_2PO_4^- + {}^{\bullet}OH \rightarrow H_2PO_4^{\bullet} + OH^- \quad (25)$$

Nitrate ions (NO_3^-) does not exhibit significant effects on the reaction in most cases [17,18,49,59,79]. However, in the study conducted by Tayyebeh Soltani *et al.* [73], NO_3^- reacted with $SO_4^{\bullet-}$ to form nitro radicals ($NO_3^{\bullet}$) with higher redox potential (Eq. 26), which increases the rate of degradation reaction.

$$NO_3^- + SO_4^{\bullet-} \rightarrow NO_3^{\bullet} + SO_4^{2-} \quad (26)$$

Similar to NO_3^-, the bromate ions (BrO_3^-) in the solution can generate more active bromate radicals ($BrO_2^{\bullet}$) (Eq. 27), thereby increasing the reaction rate [73].

$$BrO_3^- + 2H^+ + e^- \rightarrow BrO_2^{\bullet} + H_2O \quad (27)$$

Sulfate ions (SO_4^{2-}) in the solution exhibited no significant effect on the reaction in different reaction systems [58,59,79,86].

(2) Natural organic matter: Humic acid (HA), a respective natural organic matter (NOM) in wastewater, exhibited significant inhibition on the reaction system at different concentrations [58,59,67,72]. HA competes with the target pollutant and consumes ROS in solution. Besides, HA combines with the active sites of the catalyst, hindering the interaction between perovskite and oxidant and reducing the production of free radicals [67].

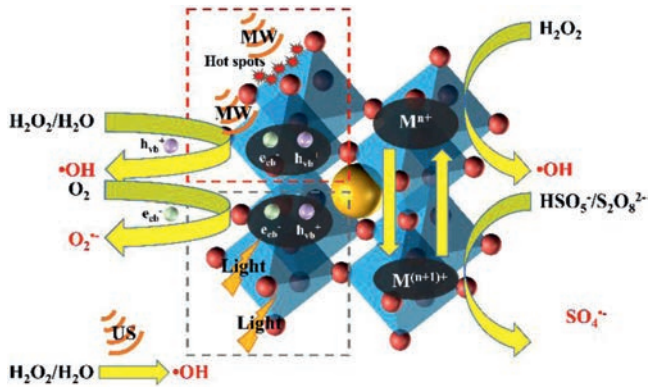

Fig. 1. Proposed mechanism of peroxides activation on perovskite catalysts: Transition metal redox, light/ultrasound/microwave activation.

4. Mechanism of activation reactions

4.1. Transition metal activation

As shown in Fig. 1, the single-electron transfer that takes place between the oxidant and the transition metal is the primary mechanism by which the perovskites activate the oxidant to generate ROS.

Firstly, oxidants combine with the active sites on the perovskite surface. Subsequently, electron transfer occurs, and the redox cycle is completed. Detailed processes of activation are as follows: Low-valence transition metals (M^{n+}) donates one electron and oxidize itself to a high-valence state ($M^{(n+1)+}$). Oxidants (HSO_5^-, H_2O_2, and $S_2O_8^{2-}$) receive this electron and generate the dominant free radicals ($SO_4^{\bullet-}$ and $^{\bullet}OH$) (Eqs. 28-30).

$$M^{n+} + HSO_5^- \rightarrow M^{(n+1)+} + SO_4^{\bullet-} + OH^- \quad (28)$$

$$M^{n+} + H_2O_2 \rightarrow M^{(n+1)+} + {}^{\bullet}OH + OH^- \quad (29)$$

$$M^{n+} + S_2O_8^{2-} \rightarrow M^{(n+1)+} + SO_4^{\bullet-} + SO_4^{2-} \quad (30)$$

In order to complete the redox cycle, $M^{(n+1)+}$ needs to accept one electron and be reduced to M^{n+} again. Among different oxidants, HSO_5^- and H_2O_2 can directly donate an electron to $M^{(n+1)+}$ and generate other free radicals ($SO_5^{\bullet-}$ and $HO_2^{\bullet}$) at the same time (Eqs. 31 and 32). However, $S_2O_8^{2-}$ cannot be used as an electron donor. In other words, the redox cycle cannot be completed by $S_2O_8^{2-}$ alone [88]. Only when $M^{(n+1)+}$ captures electrons in other ways can it be reduced to M^{n+} again (Eq. 33).

$$M^{(n+1)+} + HSO_5^- \rightarrow M^{n+} + SO_5^{\bullet-} + H^+ \quad (31)$$

$$M^{(n+1)+} + H_2O_2 \rightarrow M^{n+} + HO_2^{\bullet} + H^+ \quad (32)$$

$$M^{(n+1)+} + e^- \rightarrow M^{n+} \quad (33)$$

Besides the redox cycle, there are some side reactions. In PMS or PDS systems, $SO_4^{\bullet-}$ can further react with H_2O or OH^- to form $^{\bullet}OH$ (Eqs. 34 and 35). $SO_5^{\bullet-}$ can self-decompose into $SO_4^{\bullet-}$ and O_2 (Eq. 36).

$$SO_4^{\bullet-} + H_2O \rightarrow {}^{\bullet}OH + SO_4^{2-} + H^+ \quad (34)$$

$$SO_4^{\bullet-} + OH^- \rightarrow {}^{\bullet}OH + SO_4^{2-} \quad (35)$$

$$2SO_5^{\bullet-} \rightarrow 2SO_4^{\bullet-} + O_2 \quad (36)$$

In the H_2O_2 reaction system, $^{\bullet}OH$ can also attack H_2O_2 molecules to produce $HO_2^{\bullet}$, Eq. 37). $HO_2^{\bullet}$ can further react with $M^{(n+1)+}$ and M^{n+} to produce O_2 and HO_2^- respectively (Eqs. 38 and 39) [48]. When more than one type of transition metal ion participates in the reaction, synergistic effects may occur between different ions (such as the reduction of Fe^{3+} by Cu^+).

$$^{\bullet}OH + H_2O_2 \rightarrow HO_2^{\bullet} + H_2O \quad (37)$$

$$M^{(n+1)+} + HO_2^{\bullet} \rightarrow M^{n+} + O_2 + H^+ \quad (38)$$

$$M^{n+} + HO_2^{\bullet} \rightarrow M^{(n+1)+} + HO_2^- \quad (39)$$

4.2. Oxygen vacancy activation

Oxygen vacancies exist on the surface of perovskites. Current studies find the contribution of oxygen vacancies to activation mainly in PMS and H_2O_2 reaction systems.

In both PMS and H_2O_2 systems, oxygen vacancies can be used as defective sites to promote the formation of chemical bonds between perovskites and oxidants, which is beneficial to complete the redox cycle from $M^{(n+1)+}$ to M^{n+} (Eqs. 40-43). Meanwhile, oxygen vacancies can affect the electron asymmetrical chemical states of metals and enhance the activity of the catalytic sites [10,18,87].

$$M^{n+} + HSO_5^- + V_o^{\bullet\bullet} \rightarrow M^{(n+1)+} + SO_4^{\bullet-} + H^+ + O_o^{\times} \quad (40)$$

$$M^{(n+1)+} + HSO_5^- + H^+ + O_o^{\times} \rightarrow M^{n+} + SO_5^{\bullet-} + H_2O + V_o^{\bullet\bullet} \quad (41)$$

$$M^{n+} + H_2O_2 + V_o^{\bullet\bullet} \rightarrow M^{(n+1)+} + {}^{\bullet}OH + H^+ + O_o^{\times} \quad (42)$$

$$M^{(n+1)+} + H_2O_2 + O_o^{\times} \rightarrow M^{n+} + H_2O + {}^1O_2 \quad (43)$$

where $V_o^{\bullet\bullet}$ represents a doubly charged oxygen vacancy on the surface of perovskite, and $O_o^{\times}$ represents an oxygen ion in the vacancy.

Distinguishingly, in the PMS system, some studies [17,58] show that oxygen vacancy $V_o^{\bullet\bullet}$ can be easily converted into $^1O_2$ (Eqs. 44 and 45). In another study [57], oxygen vacancies did not directly participate in the production of $^1O_2$ but reduced the activation energy of the process (Eq. 46).

$$V_o^{\bullet\bullet} \rightarrow O_o^{\times} \quad (44)$$

$$O_o^{\times} + HSO_5^- \rightarrow HSO_4^- + {}^1O_2 \quad (45)$$

$$HSO_5^- + SO_5^{2-} \rightarrow SO_4^{2-} + HSO_4^- + {}^1O_2 \quad (46)$$

In the H_2O_2 system, oxygen vacancies provided other ways to generate $^{\bullet}OH$. Since oxygen vacancies are rich in electrons, H_2O_2 molecules on it may have longer O-O bond length, which makes it easier to decompose to $^{\bullet}OH$. Besides, oxygen vacancies also adsorb H_2O and promote its decomposition (Eqs. 47 and 48) [89].

$$V_o^{\bullet\bullet} + H_2O_2 \rightarrow {}^{\bullet}OH + OH^- \quad (47)$$

$$V_o^{\bullet\bullet} + H_2O \rightarrow {}^{\bullet}OH + H^+ \quad (48)$$

4.3. Energy input activation

(1) Light irradiation: Light irradiation is widely combined with Fenton or Fenton-like reactions. Under the irradiation of light, the photoelectron-hole pairs will be generated on the catalysts (Eq. 49) [90-92]. Wherein, photoelectrons (e_{cb}^-) can participate in the redox cycle [93] and react with H_2O_2 to form $^{\bullet}OH$ (Eqs. 50 and 51). Electron holes (h_{vb}^+) can oxidize pollutants directly and produce $^{\bullet}OH$ radicals by reacting with OH^- or H_2O (Eqs. 52 and 53) [51,53,66,73,94,95].

$$ABO_3 + hv \rightarrow e_{cb}^- + h_{vb}^+ \quad (49)$$

$$M^{(n+1)+} + e_{cb}^- \rightarrow M^{n+} \quad (50)$$

$$e_{cb}^- + H_2O_2 \rightarrow {}^{\bullet}OH + OH^- \quad (51)$$

$$h_{vb}^+ + H_2O \rightarrow {}^{\bullet}OH + H^+ \quad (52)$$

$$h_{vb}^+ + OH^- \rightarrow {}^{\bullet}OH \quad (53)$$

Where *hv* represents the induce of visible light, UV light or other form of light irradiation.

(2) Ultrasound: Ultrasonic-assisted Fenton reactions have received increasing attention in recent years. Ultrasound forms tiny bubbles in water through acoustic cavitation. Bubbles generate, grow, and collapse in a short period of time and release a large amount of energy within a small area, causing the phenomenon of sonoluminescence and local hot spots. Such conditions promote the production of free radicals.

With the help of ultrasound, H_2O_2 can be produced from water. Firstly, water is decomposed into $^{\bullet}OH$ and $^{\bullet}H$ by the ultrasound-caused local spots (Eq. 54). Then, these radicals tend to combine to form more stable substances (H_2O, H_2 and H_2O_2) (Eqs. 55-57). H_2O_2 continues to interact with the catalyst, and the traditional Fenton reaction occurs. At the same time, the sonoluminescence phenomenon leads to the production of photoelectrons, which further react to generate $^{\bullet}OH$ (Eq. 58) [85,95]. As for the H_2O_2 in the solution, ultrasound can also decompose them to produce $^{\bullet}OH$ (Eq. 59).

$$H_2O +))) \rightarrow {}^{\bullet}OH + {}^{\bullet}H \quad (54)$$

$$^{\bullet}OH + {}^{\bullet}H \rightarrow H_2O \quad (55)$$

$$^{\bullet}H + {}^{\bullet}H \rightarrow H_2 \quad (56)$$

$$^{\bullet}OH + {}^{\bullet}OH \rightarrow H_2O_2 \quad (57)$$

$$3e^- + O_2 + 2H^+ \rightarrow {}^{\bullet}OH + OH^- \quad (58)$$

$$H_2O_2 +))) \rightarrow {}^{\bullet}OH + {}^{\bullet}OH \quad (59)$$

Where))) represents the induce of ultrasound.

(3) Electrical energy: Electrochemical advanced oxidation processes (EAOPs) mainly oxidize pollutants by *in situ* electrochemically generated $^{\bullet}OH$ [96]. The anodicoxidation (AO) is one of the most widely used EAOPs. Water molecules are adsorbed to the surface of the anode (E) and are oxidized to generate $^{\bullet}OH$. The electric Fenton process (EF) is a combination of the AO and Fenton reaction. EF generates $^{\bullet}OH$ in two ways: One is the AO mentioned above (Eq. 60). Another is to reduce the dissolved oxygen at cathode in acidic medium to *in situ* produce H_2O_2 (Eq. 61). Then the traditional Fenton reaction is carried out. And at the same time, cathode helps to reduce transition metal ions to complete the redox cycle (Eq. 33) [81].

$$E + H_2O \rightarrow E(^{\bullet}OH) + H^+ + e^- \quad (60)$$

$$O_2 + 2H^+ + 2e^- \rightarrow H_2O_2 \quad (61)$$

Where E represents the anode of electrochemical system, E($^{\bullet}OH$) represents the hydroxyl radicals generated on the anode surface.

(4) Microwave: Some recent studies have reported perovskite-based microwave-induced catalytic oxidation (MICO) [52,54]. It has been proven that in such systems free radical still plays a major role, input microwave (MW) asissted the reactions. Firstly, the perovskites could absorb microwave energy and form many hot spots on its surface, which can directly degrade pollutants Eq. 62). More importantly, microwaves can stimulate the catalysts to generate electron-hole (e_{cb}^--h_{vb}^+) pairs on the surface (Eq. 63). Similar to the photocatalytic process, the generated e_{cb}^- not only promote the reduction reaction of transition metals, but it also reacts with O_2/H_2O_2 to generate $O_2^{\bullet-}/{}^{\bullet}OH$ (Eqs. 64 and 51). The generated h_{vb}^+ can react with water/OH^- to generate $^{\bullet}OH$ (Eqs. 52 and 53). In addition, the oxidant (H_2O_2) can also absorb the energy of microwaves and generate more $^{\bullet}OH$ (Eq. 65).

$$ABO_3 + MW \rightarrow ABO_3(\text{hotspots}) \quad (62)$$

$$ABO_3 + MW \rightarrow e_{cb}^- + h_{vb}^+ \quad (63)$$

$$e_{cb}^- + O_2 \rightarrow O_2^{\bullet-} \quad (64)$$

$$H_2O_2 + MW \rightarrow {}^{\bullet}OH + {}^{\bullet}OH \quad (65)$$

Where MW represents the induce of microwave.

5. Summary and prospects

In this review, we have evaluated recent studies on the application of perovskite in wastewater advanced oxidation processes. Overall, perovskite catalysts demonstrated good catalytic activity and significantly improved the efficiency of AOPs. In order to further improve the efficiency of perovskite-based AOPs, many methods have been implemented, including material modification (such as metal doping and material compounding) and energy input (light irradiation, ultrasound, electricity, and microwave). With the help of perovskites, a large amount of ROS (mainly $SO_4^{\bullet-}$, $^{\bullet}OH$, $^1O_2$, *etc.*) are produced *in situ*, which play the most important role in the degradation of pollutants.

Factors affecting reaction efficiency include reaction temperature, initial pH, oxidant concentration, catalyst dosage and the presence of co-existing compounds. Wherein, high temperature can accelerate the diffusion and adsorption of pollutants and provide more energy for the cleavage of the peroxide O−O bond, which always has a positive effect. Initial pH can affect the type and concentration of free radicals, the surface charge of the catalyst, the existing form of oxidants and pollutants, and the amount of metal leaching. Under the influence of both positive and negative aspects, the effect of initial pH did not show a specific rule. Increasing peroxide and catalyst dosage can provide more precursors and active sites for ROS production. However, the excessive peroxide will lead to the quenching of ROS and too much catalyst will lead to aggregation and subsequently reduce the surface area, which limits the improvement of the degradation efficiency. Therefore, the increase in oxidant concentration and catalyst dosage can

improve the reaction efficiency to a certain extent, but there are limitations. Co-existing compounds include various anions and natural organic matter. In general, the promotion results from the production of more active ROS. The inhibition is not only caused by the production of less active radicals but also the combination of co-existing compounds and the catalyst surface. It is noteworthy that the effect of the co-existing compounds on reaction efficiency is more pronounced at higher concentrations.

The most important mechanism of perovskite-based AOPs is the single-electron transfer between the transition metal and the peroxide. A redox cycle is completed, and a large amount of ROS is produced in the process. Besides, oxygen vacancies on the perovskite surface can effectively promote the redox cycle. There are several different forms of energy input (light, ultrasound, electricity, and microwave) to assist the reaction. Light irradiates on the perovskite to produce the photoelectron/electron-hole pair. Ultrasound generates tiny cavitation bubbles in the solution which will collapse and release a large amount of energy. The resulting phenomenon of sonoluminescence and local hot spots promote the generation of ROS. The input of electrical energy makes anodic oxidation combine with Fenton reactions and form an electric Fenton reaction. The introduction of microwaves generate hot spots on the surface of perovskite which assists the reaction. More importantly, microwaves can also excite electron-hole pairs on the perovskite surface which can promote the generation of free radicals.

Based on the review of the achievements so far and the discovery of the existing problems, we propose some prospects for the future application of perovskite oxides in wastewater treatment.

(1) The optimum pH is quite different in perovskite-based AOPs. In terms of environmental friendliness, operability, and processing costs, the reaction conditions close to the natural environment are the most ideal. Therefore, the perovskites that can exert the strongest catalytic effect under neutral pH conditions and efficiently degrade pollutants deserve more attention.
(2) Recyclability is one of the indispensable indicators for evaluating the perovskite catalyst. To realize the recovery of the perovskite, it must first be separated from the wastewater. One possible method is to choose magnetic materials as catalysts. Thus, the development of perovskite catalysts with magnetism can be considered in subsequent work.
(3) Many current studies improved the effect of AOPs in degrading pollutants by inputting different forms of energy to the system. However, it cannot be ignored that this method has high requirements for equipment and energy. Due to the low bandgap energy of perovskites, it can be activated by visible light. Therefore, assistance from solar energy should be incorporated for the activation of perovskites to decrease energy input and lower processing costs.
(4) In most perovskite-based AOPs, free radicals are the main ROS. The interference of coexisting compounds on the reaction is mainly attributed to the quenching of free radicals. Correspondingly, in the AOPs that produce non-radical ROS (such as $^1O_2$), co-existing ions show a less significant effect on it [18,57-59]. It is feasible for future studies to establish more perovskite-based AOPs dominated by $^1O_2$ which can avoid interference to a great extent.
(5) The current studies mainly focus on the degradation efficiency of perovskite-based AOPs. However, the environmental toxicological effects of reaction by-products and the perovskite material itself have not been adequately studied. Therefore, more attention should be placed on this aspect in the future to ensure environmental and biological safety.

Declaration of competing interest

The authors declare that they have no known competing financial interests or personal relationships that could have appeared to influence the work reported in this paper.

Acknowledgments

The authors would like to acknowledge the financial support from National Key R&D Program of China (No. 2019YFD1100200), National Natural Science Foundation of China (Nos. 51878431, 51961145106), Shanghai Rising-Star Program (No. 20QC1401200), Shanghai Science and Technology Committee (No. 19DZ1208400), and State Key Laboratory of Pollution Control and Resource Reuse Foundation, (No. PCRRE20002).

References

[1] F. Ghanbari, M. Moradi, Chem. Eng. J. 310 (2017) 41–62.
[2] X. Duan, C. Su, J. Miao, Appl. Catal. B: Environ. 220 (2018) 626–634.
[3] J. Wang, S. Wang, Chem. Eng. J. 334 (2018) 1502–1517.
[4] J.L. Wang, L.J. Xu, Crit. Rev. Environ. Sci. Technol. 42 (2012) 251–325.
[5] S. Yang, P. Wang, X. Yang, J. Hazard. Mater. 179 (2010) 552–558.
[6] J. Chen, C. Fang, W. Xia, T. Huang, C.H. Huang, Environ. Sci. Technol. 52 (2018) 1461–1470.
[7] J. Chen, L. Zhang, T. Huang, J. Hazard. Mater. 320 (2016) 571–580.
[8] H. Gao, J. Chen, Y. Zhang, X. Zhou, Chem. Eng. J. 306 (2016) 522–530.
[9] J. Chen, X. Zhou, P. Sun, Y. Zhang, C.H. Huang, Environ. Sci. Technol. 53 (2019) 11774–11782.
[10] C. Su, X. Duan, J. Miao, ACS Catal. 7 (2017) 388–397.
[11] H. Zhang, S. Cheng, B. Li, X. Cheng, Q. Cheng, Sep. Purif. Technol. 202 (2018) 242–247.
[12] K.A. Lin, Y. Chen, Y. Lin, Chem. Eng. Sci. 160 (2017) 96–105.
[13] H. Zhang, Q. Ji, L. Lai, G. Yao, B. Lai, Chin. Chem. Lett. 30 (2019) 1129–1132.
[14] X. Jiang, Y. Guo, L. Zhang, W. Jiang, R. Xie, Chem. Eng. J. 341 (2018) 392–401.
[15] X. Wang, X. Pu, Y. Yuan, Chin. Chem. Lett. 31 (2020) 2634–2640.
[16] S. Zou, Q. Chen, Y. Liu, Chin. Chem. Lett. 32 (2021) 2066–2072.
[17] M. Zhu, J. Miao, X. Duan, ACS Sustain. Chem. Eng. 6 (2018) 15737–15748.
[18] J. Li, J. Miao, X. Duan, Adv. Funct. Mater. 28 (2018) 1804654.
[19] G. Wang, C. Cheng, J. Zhu, Sci. Total Environ. 673 (2019) 565–575.
[20] Z. Mo, H. Chen, K. Wang, Z. Shi, H. Li, Chin. Chem. Lett. 15 (2004) 721–724.
[21] W.H. Yuan, C.S. Dong, L. Li, Chin. Chem. Lett. 23 (2012) 957–960.
[22] Z. Zhong, Q. Liang, Q. Yan, X. Fu, Chin. Chem. Lett. 6 (1995) 167–168.
[23] A. Anantharaman, B.A. Josephine, V.M. Teresita, T. Ajeesha, M.o.N.N. George, J. Nanosci. Nanotechnol. 19 (2019) 5116–5129.
[24] P. Garcia-Muñoz, C. Lefevre, D. Robert, N. Keller, Appl. Catal. B: Environ. 248 (2019) 120–128.
[25] S.Z. Tan, L.C. Ding, Y.L. Liu, Y.S. Ouyang, Y.B. Chen, Chin. Chem. Lett. 18 (2007) 85–88.
[26] X. Pang, Y. Guo, Y. Zhang, B. Xu, F. Qi, Chem. Eng. J. 304 (2016) 897–907.
[27] Z.N. Garba, W. Zhou, M. Zhang, Z. Yuan, Chemosphere 244 (2019) 125474.
[28] Z.P. Shao, G.T. Li, G.X. Xiong, W.S. Yang, Chin. Chem. Lett. 11 (2000) 1103–1106.
[29] G.L. Yang, H.Z. Zhong, Chin. Chem. Lett. 27 (2016) 1124–1130.
[30] L.G. Tejuca, J.L.G. Fierro, J.M.D. Tascón, Structure and reactivity of perovskite–type oxides, in: D.D. Eley, H. Pines, P.B. Weisz (Eds.), Advances in Catalysis, Academic Press, Inc., 1989, pp. 237–328.
[31] M.A. Peña, J.L.G. Fierro, Chem. Rev. 101 (2001) 1981–2018.
[32] V.M. Goldschmidt, Naturwissenschaften 14 (1926) 477–485.
[33] R.E. Cohen, Nature 358 (1992) 136–138.
[34] R. Seshadri, N.A. Hill, Chem. Mater. 13 (2001) 2892–2899.
[35] R. Sun, C. He, L. Fu, Chin. Chem. Lett. (2021), doi:10.1016/j.cclet.2021.05.072.
[36] I.A. Sergienko, E. Dagotto, Phys. Rev. B: Condens. Matter Mater. Phys. 73 (2006) 094434.
[37] P. Baettig, C.F. Schelle, R. LeSar, U.V. Waghmare, N.A. Spaldin, Chem. Mater. 17 (2005) 1376–1380.
[38] Y. Chen, S. Lan, M. Zhu, Chin. Chem. Lett. 32 (2021) 2052–2056.
[39] A. Bhalla, R. Guo, R. Roy, Mater. Res. Innovations 4 (2000) 3–26.
[40] J. Yu, C. He, C. Pu, Chin. Chem. Lett. 32 (2001) 3149–3154.
[41] J. Hwang, R.R. Rao, L. Giordano, Science 358 (2017) 751–756.
[42] H. Yang, C. He, L. Fu, Chin. Chem. Lett. 32 (2001) 3202–3206.
[43] E. Grabowska, Appl. Catal. B: Environ. 186 (2016) 97–126.
[44] R. Wang, C. He, W. Chen, C. Zhao, J. Huo, Chin. Chem. Lett. (2021), doi:10.1016/j.cclet.2021.05.024.
[45] K.A. Lin, Y. Chen, T. Lin, H. Yang, J. Colloid Interface Sci. 497 (2017) 325–332.
[46] K.A. Lin, T. Lin, Y. Lu, J. Lin, Y. Lin, Chem. Eng. Sci. 168 (2017) 372–379.
[47] T. Ma, L. Liu, B. Meng, Sep. Purif. Technol. 211 (2019) 298–302.
[48] S.B. Hammouda, F. Zhao, Z. Safaei, Appl. Catal. B: Environ. 218 (2017) 119–136.
[49] R. Zhang, Y. Wan, J. Peng, Chem. Eng. J. 372 (2019) 796–808.
[50] L.G. Devi, B. Anitha, Surf. Interfaces 11 (2018) 48–56.
[51] K. Wang, H. Niu, J. Chen, Appl. Surf. Sci. 404 (2017) 138–145.
[52] Y. Wang, L. Yu, R. Wang, Y. Wang, X. Zhang, J. Colloid Interface Sci. 574 (2020) 74–86.

[53] T.T.N. Phan, A.N. Nikoloski, P.A. Bahri, D. Li, Appl. Surf. Sci. 491 (2019) 488–496.
[54] Y. Wang, R. Wang, L. Yu, Chem. Eng. J. 401 (2020) 126057.
[55] R.R. Solís, F.J. Rivas, O. Gimeno, J.L. Pérez-Bote, J. Chem. Technol. Biotechnol. 92 (2017) 2159–2170.
[56] S. Hu, Y. Yu, Y. Guan, Chin. Chem. Lett. 31 (2020) 2839–2842.
[57] P. Gao, X. Tian, Y. Nie, Chem. Eng. J. 359 (2019) 828–839.
[58] J. Miao, X. Duan, J. Li, Chem. Eng. J. 355 (2019) 721–730.
[59] X. Tian, P. Gao, Y. Nie, Chem. Commun. 53 (2017) 6589–6592.
[60] Y. Chu, X. Tan, Z. Shen, J. Hazard. Mater. 356 (2018) 53–60.
[61] M. Zhu, J. Miao, D. Guan, ACS Sustain. Chem. Eng. 8 (2020) 6033–6042.
[62] S. Lu, G. Wang, S. Chen, J. Hazard. Mater. 353 (2018) 401–409.
[63] C. Cheng, S. Gao, J. Zhu, Chem. Eng. J. 384 (2020) 123377.
[64] X. Li, M. Li, X. Ma, Chem. Eng. Sci. 219 (2020) 115596.
[65] J. Miao, J. Sunarso, C. Su, Sci. Rep. 7 (2017) 44215.
[66] F. Chi, B. Song, B. Yang, RSC Adv. 5 (2015) 67412–67417.
[67] J. Miao, J. Sunarso, X. Duan, J. Hazard. Mater. 349 (2018) 177–185.
[68] M. Ghiasi, A. Malekzadeh, Sep. Purif. Technol. 134 (2014) 12–19.
[69] H. Guo, X. Zhou, Y. Zhang, J. Environ. Sci. (China) 91 (2020) 10–21.
[70] M.R. Carrasco-Díaz, E. Castillejos-López, A. Cerpa-Naranjo, M.L. Rojas-Cervantes, Chem. Eng. J. 304 (2016) 408–418.
[71] K.A. Lin, T. Lin, Water, Air, Soil Pollut. 229 (2018) 10.
[72] S.B. Hammouda, F. Zhao, Z. Safaei, Appl. Catal. B: Environ. 233 (2018) 99–111.
[73] T. Soltani, A. Tayyebi, B.-K. Lee, Appl. Surf. Sci. 441 (2018) 853–861.
[74] K. Rusevova, R. Köferstein, M. Rosell, Chem. Eng. J. 239 (2014) 322–331.
[75] B. Palas, G. Ersöz, S. Atalay, Process Saf. Environ. Prot. 111 (2017) 270–282.
[76] O.P. Taran, A.B. Ayusheev, O.L. Ogorodnikova, Appl. Catal. B: Environ. 180 (2016) 86–93.
[77] S.B. Hammouda, F. Zhao, Z. Safaei, Appl. Catal. B: Environ. 215 (2017) 60–73.
[78] R.R. Solís, F.J. Rivas, O. Gimeno, Appl. Catal. B: Environ. 200 (2017) 83–92.
[79] Y. Rao, F. Han, Q. Chen, Chemosphere 218 (2019) 299–307.
[80] A. Aizat, F. Aziz, M.N.M. Sokri, SN Appl. Sci. 1 (2019) 91.
[81] S.B. Hammouda, C. Salazar, F. Zhao, Appl. Catal. B: Environ. 240 (2019) 201–214.
[82] M. Dükkancı, Water Sci. Technol. 79 (2019) 386–397.
[83] L. Zhang, Y. Nie, C. Hu, J. Qu, Appl. Catal. B: Environ. 125 (2012) 418–424.
[84] J. Mao, X. Quan, J. Wang, Front. Environ. Sci. Eng. 12 (2018) 10.
[85] S.G. Babu, P. Aparna, G. Satishkumar, M. Ashokkumar, B. Neppolian, Ultrason. Sonochem. 34 (2017) 924–930.
[86] Y. Nie, L. Zhang, Y.-Y. Li, C. Hu, J. Hazard. Mater. 294 (2015) 195–200.
[87] Y. Rao, Y. Zhang, F. Han, Chem. Eng. J. 352 (2018) 601–611.
[88] G.P. Anipsitakis, D.D. Dionysiou, Environ. Sci. Technol. 38 (2004) 3705–3712.
[89] H. Wang, L. Zhang, C. Hu, Chem. Eng. J. 332 (2018) 572–581.
[90] H. Zhang, J. He, C. Zhai, M. Zhu, Chin. Chem. Lett. 30 (2019) 2338–2342.
[91] J. Hu, C. Zhai, M. Zhu, Chin. Chem. Lett. 32 (2021) 1348–1358.
[92] M. Zhang, J. He, Y. Chen, Chin. Chem. Lett. 31 (2020) 2721–2724.
[93] Y. Zhu, T. Wang, W. Wang, Environ. Chem. Lett. 17 (2019) 481–486.
[94] M. Dükkancı, Turk. J. Chem. 40 (2016) 784–801.
[95] M. Dükkancı, Ultrason. Sonochem. 40 (2018) 110–116.
[96] J. Li, Y. Li, Z. Xiong, G. Yao, B. Lai, Chin. Chem. Lett. 30 (2019) 2139–2146.